Available online at www.sciencedirect.com
SCIENCE DIRECT®
Polymer 44 (2003) 7765–7776
polymer
www.elsevier.com/locate/polymer

Investigation of the effect of chain rigidity on orientation of polymer blends: the case of poly(vinyl phenol)/poly(ethylene terephthalate) blends

Patricia Gestoso, Josée Brisson*

CERSIM, Département de chimie, Faculté de sciences et de génie, Université Laval, Pavillon Vachon, Québec, Qué., Canada G1K 7P4

Received 25 June 2003; received in revised form 29 September 2003; accepted 29 September 2003

Abstract

Orientation of amorphous, miscible poly(vinyl phenol) (PVPh)-poly(ethylene terephthalate) (PET) blends is studied using experimental and modelling techniques. Up to 50 wt% PVPh, the blends are semi-crystalline and were therefore not studied. At 60 wt% PVPh, no crystallisation was observed using either differential scanning calorimetry or X-ray diffraction. For the 60wt% PVPh blend, FTIR dichroism determination showed that orientation was relatively high (0.09 at a $\lambda = 3.4$) and similar for both polymers. Above 60 wt% PVPh, however, no appreciable orientation was detected. In order to gain insights about the deformation phenomena in polymer blends, atomistic models of the 60 wt% PVPh composition were built using the Meirovitch approach. These were found in good agreement with X-ray diffraction, and exhibit a fair degree of interpenetration as estimated visually and by comparing intermolecular pair distribution functions. Significant hydrogen bonding was found: 8% of carbonyl oxygens and 1% of carboxylate oxygens of PET are bound to PVPh. Deformation simulations were performed using the Parrinello–Rahman deformation scheme. Orientation of PVPh and PET in the blend was found equivalent to that observed in pure polymers simulations. PET orientation followed the aggregate model and was more oriented than PVPh by a factor of two. It was concluded that the similarity in orientation of the two polymers in the blend, which was observed experimentally on quenched samples, could be due to a combination of different deformation-induced orientation followed by distinct relaxation mechanism and relaxation times for both polymers.

Keywords: Orientation; Infrared; Simulation

1. Introduction

In spite of its profound influence on material properties, orientation of polymer blends still remains difficult to predict or even understand. Measured orientation results from two concurrent phenomena: induced deformation and chain relaxation. It is relatively easy to follow the later stages of relaxation by dynamics methods such as birefringence [1] or polarization-modulation infrared linear dichroism [2–5], but it is still impossible to remove completely the effect of relaxation from deformation measurements, due to the timescale limits of the various techniques used. Proposed deformation models therefore still lack, to a great extent, experimental validation.

When interpreting orientation measurements in blends, deformation-induced differences between the two polymers is rarely invoked, and discussion is either centered on relaxation-induced differences, or on parameters which could be incorporated in models of both deformation and relaxation. Such parameters include the χ interaction parameter [6], chain tortuosity [7] or incipient phase separation [8].

Our group has focussed for a number of years on hydrogen bond forming blends based on poly(vinyl phenol), abbreviated PVPh. This polymer was chosen for its ability to form hydrogen bonds with a large number of polymers, as these interactions are amenable to qualitative or semi-quantitative estimation through infrared spectroscopy. Orientation of blends with poly(methyl methacrylate) [9], poly(ethylene oxide) [10] and poly(vinyl methyl ether) [11] were previously studied. In parallel, molecular modelling simulations of the orientation phenomena in pure polymers were undertaken, with the aim of getting insights on the deformation mechanism, which cannot be isolated experimentally from relaxation. PET deformation was shown to

* Corresponding author. Tel.: +1-418-656-3536; fax: +1-418-656-7916.
E-mail address: josee.brisson@chm.ulaval.ca (J. Brisson).

0032-3861/$ - see front matter © 2003 Elsevier Ltd. All rights reserved.
doi:10.1016/j.polymer.2003.09.058

behave as predicted by the pseudo-affine or aggregate model, which neglects changes in lengths or the units and simply considers orientation of rigid segments [12,13]. On the other hand, poly(vinyl phenol) (PVPh) deviates significantly from this model. This was attributed to the relative flexibility of its backbone, which is composed solely of methylene units [14]. This suggests that the initial orientation developed in a pure amorphous polymer is related, at least in part, to the intrinsic rigidity of the repeat unit, as tentatively defined by the number of rotatable bonds which contribute to changes in the relative length of the backbone.

In the present work, we aim at investigating the effect of backbone chain rigidity on orientation of a polymer blend. The system chosen for this purpose is the PVPh-PET blend, which has previously been reported to be miscible [15] and for which experimental [16] and atomistic modelling experiments have already been performed for both pure polymers [17,18]. Experimental investigations using FTIR dichroism will be coupled to molecular modelling simulations of the deformation process in order to gain insights on the orientation of a polymer blend for which the two components differ in chain rigidity.

2. Methodology

2.1. Experimental

Poly(vinyl phenol) (PVPh) was purchased through Polysciences Inc., and was found to have a weight-average molecular weight M_w of 5200 g mol^{-1} and polydispersity index of 2.3 by gel permeation chromatography measurements. Poly(ethylene terephthalate) (PET) was supplied by Du Pont with M_w of 54,600 g mol^{-1} and polydispersity index of 1.9, as determined by size exclusion chromatography. PET-PVPh blends were prepared by placing the polymers in powder form in a MiniMax blender model CS-183 at 254 °C. Glass transition temperatures T_g and melting points T_m are reported in Table 1 and Fig. 1 and were measured using a Perkin Elmer DSC-7 at a heating rate of 10 °C/min. T_g were determined as the midpoint of the transition. Temperature was calibrated using indium. Densities of pure PVPh and pure amorphous PET were determined by flotation in methylene chloride–propanol mixtures. Density of blends was estimated as mass average of the pure polymers.

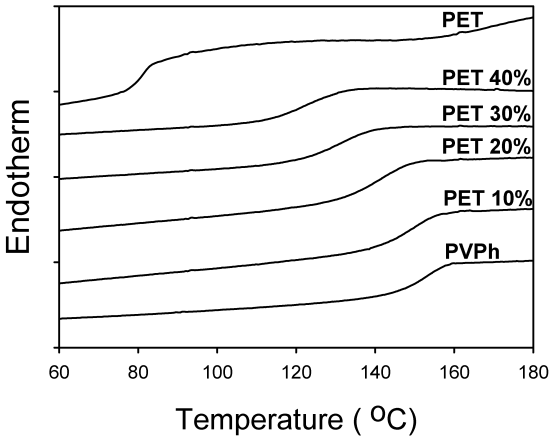

Fig. 1. Differential scanning calorimetry (10 °C/min) of PVPh-PET blends.

Blend films were compressed at $T_g + 55$ °C and cut into 15 × 10 mm strips. Drawing of films was performed at an exponential stretching rate of 0.1 s^{-1} and a temperature of $T_g + 17$ °C in a custom-made stretcher. Due to high brittleness of samples, lower temperatures invariably led to sample breakage. Before drawing, samples were kept at the stretching temperature for a period ranging from 20 to 45 min to allow thermal equilibration. They were quenched to room temperature after stretching and prior to their removal from the stretcher using an air-fan fed with liquid nitrogen vapors.

X-ray diffraction patterns were recorded on a Rigaku X-ray diffractometer, equipped with a type 200B rotating anode generator functioning at 180 mA and 45 kV using the Ni filtered Cu Kα radiation. Spectra were recorded in the $\theta - 2\theta$ geometry.

Infra-red dichroism measurements were performed using a Nicolet Magna-IR® 560 equipped with a MCT/A detector and a polarizer. For each spectrum, 200 scans were taken at a resolution of 4 cm^{-1}. Oriented films were rotated by 90° to obtain the spectra parallel and perpendicular to the draw direction of the sample. Measured absorbances were used to calculate the dichroic ratio $R = A_{\parallel}/A_{\perp}$. In all cases, care was taken to select spectra for which absorbance of the bands of interest was inferior to one unit, which allowed use of the Beer–Lambert law.

For uniaxially oriented samples, the second-order

Table 1
PET-PVPh blends properties

Sample	PVPh/PET (wt%)	PVPh/PET (mol%)	PVPh/PET (mol% interacting units)	T_g (°C)	T_m (°C)
Pure PVPh	100/0	100/0	100/0	154	–
PVPh90%	90/10	93/7	87/13	149	–
PVPh80%	80/20	86/14	75/25	140	–
PVPh70%	70/30	79/21	65/35	130	–
PVPh60%	60/40	71/29	55/45	122	–
Pure PET	0/100	0/100	0/100	80	249

moment of the orientation function $\langle P_2(\cos\theta)\rangle$ was calculated using the following equation,

$$\langle P_2(\cos\theta)\rangle = \frac{(R-1)}{(R+2)}\frac{(R_o+2)}{(R_o-1)}$$

where $R_o = 2\cot^2\alpha$, α being the angle between the polymer chain axis and the dipole transition moment vector of the chosen vibration, and θ is the angle between the chain axis and the stretching direction. The brackets indicate that an average over all segments of the polymer is calculated.

PET-PVPh orientation were characterized using the peaks at 971 cm^{-1} for PET ($\alpha = 34°$) [19], corresponding to a *trans* C–O stretching vibration, and at 1882 cm^{-1}, corresponding to the overtone of C–H out of plane aromatic ring deformation, for PVPh (α estimated as 62° from data on a different vibration reported in Ref. [20]).

2.2. Model construction and validation

Molecular modelling was performed using the InsightII, Polymerizer, Amorphous_Cell and Discover 3 software packages of Accelrys Inc., installed on a Indigo II Silicon Graphics workstation and on an SGI Origin2000 processor. The polymer consistent forcefield [21] was used. This forcefield is composed of a Morse potential for bond deformation, a harmonic potential for bond angle deformation, a Fourier series for torsion angle deformation, a Lennard–Jones 6-12 potential for van der Waals interactions and a classical electrostatic term. Cross terms may also be included, but were omitted to speed up calculations. For all calculations, a cutoff distance of 9.5 Å was fixed to limit calculation time for nonbonded interactions and a quintic spline catenation function used between 9.5 Å and 10.0 Å. Pair-list updates were performed each time any atom moved more than half the buffer width. Hydrogen atoms were explicitly defined in all calculations.

Construction [18,22] and deformation simulations [12–14] of pure PVPh and pure PET models have been reported previously. The PVPh-PET models constructed here consist in one PVPh chain of 250 repeat units (30,000 g mol^{-1}) and one PET chain of 100 units (19,200 g mol^{-1}). This corresponds to a 61 wt% PVPh blend composition or 72 mol% PVPh blend composition. Models were constructed using the Meirovitch scanning method [23], in which stepwise construction of each chain is performed while alternating from one chain to the other at each repeat unit addition. The first repeat unit of PVPh and of PET are positioned in a random fashion in the cell. Six lookahead bonds were taken into account, and random sampling of the configurations used. During repeat unit additions, five substates of 40 degrees width were used, which decreases the probabilities of accidentally generating arrangements in which two atoms overlap. Due to catenation problems, the blends were first constructed at an initial density of 0.5 g cm^{-3} and compressed subsequently using constant number of particles, pressure and temperature molecular dynamics until the experimental density value of 1.21 g cm^{-3} was reached. Temperature was controlled by velocity scaling. An auto-ring-checking procedure was used to reject models presenting catenation during their construction. Resulting cells were cubic with $a = 40.37$ Å. All simulations reported here were performed under periodic boundary conditions and the minimum image convention.

Using the method described above, three amorphous structures with different conformations were successfully generated for the PVPh-PET blend. Initially constructed cells were annealed at 1000 K for 5 ps using an integration step of 0.001 ps and the Verlet velocity algorithm under the microcanonical constant number of atoms, constant volume and constant temperature (NVT) ensemble, following a method proposed in the literature [24,25]. Monitored pressures at the experimental density were in the range of 0.3–0.5 GPa, which indicates that experimental densities may be overestimated.

A coarse energy minimisation followed using the steepest descent algorithm until derivatives were less than 0.1 kcal mol^{-1}, and a conjugate gradients energy minimisation until maximum derivatives of 0.1 kcal mol^{-1} were observed. Deformation was performed using Parinello–Rahman NST deformation at a temperature of 298 K using stress tensors $S_{ii} = 5$ GPa and $S_{jj} = S_{kk} = -5$ GPa. Time required to attain a deformation ratio of 2.0 was 8 ps.

Geometrical criteria for hydrogen bond definition were a distance between the hydrogen donor and the oxygen acceptor of less than 3.0 Å and an angle between the proton acceptor, the proton and the proton donor greater than 90 degrees. As in previous studies, hydrogen bonds were classified according to the hydrogen bond acceptor: intrachain PVPh-PVPh hydrogen bonds were defined as having the oxygen acceptor in the parent chain, interchain PVPh-PVPh hydrogen bonds as having the oxygen acceptor in the surrounding PVPh chain replicates and interchain PVPh-PVME hydrogen bonds as having the oxygen acceptor in a PET chain. Intrachain hydrogen bonds were determined using InsightII, whereas other hydrogen bonds were calculated with a subroutine written by the authors.

Torsion angles were designated as *trans* for values of 180° ± 30°, *gauche* for values for values of ±60° ± 30°, and non-*trans*, non-*gauche* for values of ±120° ± 30° and 0° ± 30°. Calculated error, when reported, corresponds to that estimated using the Student test on the various models considered, with a probability level of 95%.

3. Results and discussion

3.1. Preparation of blends

In order to study PVPh-PET blend orientation, blends must first be prepared, their state of miscibility verified and their relative crystallinity or absence of crystallinity assessed. Since crystallinity induces important changes in

orientation behaviour and renders orientation quantification of the amorphous phase more problematic, the present study is limited to PVPh-PET blends with a PVPh content equal or superior to 60 wt%, for which no crystallinity was detected using either differential scanning calorimetry (DSC) or X-ray diffraction.

Melt blending was performed, as no common solvent were found, due largely to the low solubility of PET. Care was taken to limit thermal degradation by grinding the polymers prior to their melting, which allowed to reduce residence time at high temperatures. Miscibility was verified by DSC. The presence of a single T_g, intermediate to that of the pure polymers, and with a width comparable to those of the pure polymers, was taken as evidence of miscibility. The width of the transition is of particular importance, as T_g is used as a reference temperature in orientation studies. Although the PVPh-PMMA blend showing weaker interactions was found to partially phase-separate [26], in the case of strongly interacting blends (PVPh-PEO and PVPh-PVME), T_g enlargement never exceeded 4 °C. Similar orientation behaviour was therefore obtained whether using midpoint, onset of endpoint or T_g as a reference temperature. In the PVPh-PET system, as can be seen in Fig. 1, T_gs have a similar width as that of pure PVPh, which forms the major component, as expected for a blend miscible at a submicron level.

3.2. Orientation of the PET-PVPh system

A typical spectrum of a PVPh-PET blend is shown in Fig. 2. Orientation measurements require non-overlapping vibrations. Intensity must also be medium to low, in order not to require extremely thin films, which are harder to prepare and more prone to breakage during stretching. As can be seen in Fig. 2, for PVPh, the 1882 cm^{-1} vibration was selected, whereas for PET the 971 cm^{-1} vibration was used. The former is attributed to the overtone of C–H out-of-plane deformation and the latter was assigned to *trans* conformers. PET also exhibits vibrations related to *gauche* conformers or to aromatic rings, but in the present case, these overlapped too severely with PVPh to be used.

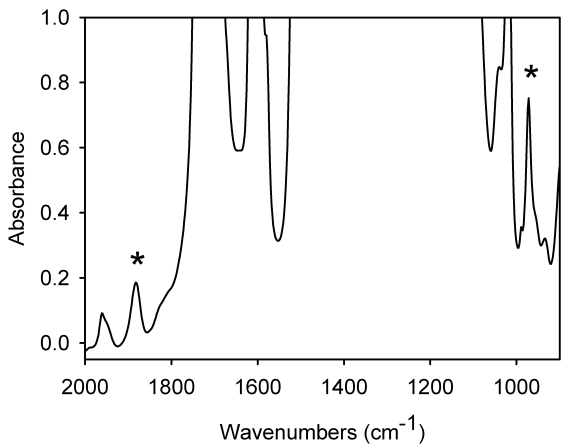

Fig. 2. Fourier transform infrared spectrum of 60 wt% PVPh blend (vibrations used for orientation measurements indicated by asterisk).

Orientation is normally calculated for the overall chain by determining the angle between a specific vibration of the repeat unit and the chain axis and averaged over all repeat units. However, for PET, no univocal chain axis can be defined. Orientation is therefore usually reported for *gauche* and *trans* segments of the glycol moiety and for aromatic cycles. For PET, *trans* segments have been shown to orient slightly more than cycles and significantly more than *gauche* segments [2]. A similar trend is expected in the blend, although due to vibration overlap, it will be impossible to verify this point.

PVPh-PET blends with PVPh percentages superior to 60 wt% surprisingly showed orientation values of zero, within experimental error, for both components, contrarily to other PVPh-based blends studied previously [9–11].This was verified by birefringence and specular reflection measurements. When the percentage of PVPh was lowered to 60 wt%, however, orientation became clearly detectable. Orientation values $\langle P_2(\cos\theta)\rangle$ for this composition are reported in Fig. 3 for PVPh and PET. Considerable data dispersion is observed, which is attributed to the low intensity of the vibrations used and to possible thermal degradation, which is suspected to occur in spite of experimental precautions taken. Orientation of PVPh and PET are comparable, within experimental error, although PVPh is, on average, slightly less oriented. Orientation varies linearly with λ for both components of the blend, contrarily to PVPh orientation in blends with PEO and with PVME, which had been attributed tentatively to changes in the relaxation regime.

Fig. 4 reports a comparison of the orientation of PVPh in blends with PET, PMMA, PEO and PVME, using the slope of the $\langle P_2(\cos\theta)\rangle$ vs λ curves, abbreviated $\Delta P_2/\Delta\lambda$. Two values are reported for PVME blends, one for a λ of 1.5 and one for 3.0, as in this case the behaviour was non-linear and

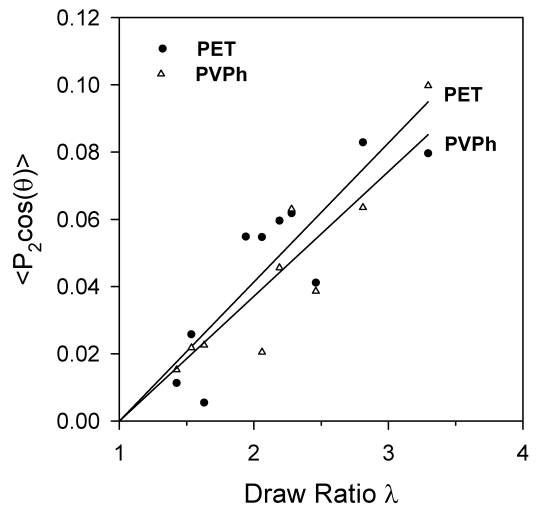

Fig. 3. Uniaxial orientation of PVPh and PET chains in PVPh 60% blends at $T_g + 17$ and 0.1 s^{-1}.

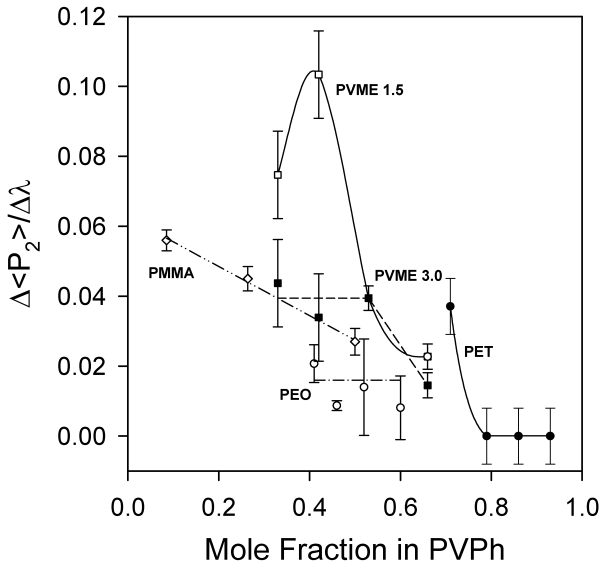

Fig. 4. Variation of $\Delta P_2/\Delta\lambda$ with composition for various PVPh-based blends. (● PEO $\lambda = 1.5$, ○ PEO $\lambda = 3.0$, □ PVME $\lambda = 1.5$, ■ PVME $\lambda = 3.0$, ▲ PET, ◇PMMA).

tangents at these specific draw ratios were used for comparison purposes. It must also be noted that PVME studies were performed using a higher molecular weight PVPh ($M_w = 29,300$ g mol^{-1} as compared to 5,200 g mol^{-1} for all other blends). Relaxation times are expected to be very different for both chains, which may therefore have been subjected to different relaxation mechanism prior to quenching. PVPh-PET blend compositions, as reported in molar fractions, are higher in PVPh than previous systems studied. Measured compositions were limited by the presence of crystallinity at higher PET concentrations. In no other case has absence of orientation been noted, which may not be conclusive since similar compositions were never studied. Pure PVPh exhibits a lower orientation ($\Delta P_2/\Delta\lambda = 0.02$ at $T_g + 15$ and a draw rate of 0.1 mm s^{-1}, as reported in reference [20]) than the 0.3 mol fraction PET blend. For the 0.71 molar fraction, PVPh orientation is in the same range as that observed for other PVPh-based blends.

The use of mole fractions in hydrogen bond systems for comparison purposes has stemmed from the idea of comparing systems on the basis of a similar number of interacting units. We use the label 'interacting unit' to define the segment within a repeat unit which is susceptible to form a hydrogen bond, that is, to be a hydrogen donor or acceptor. In the case of PMMA, PEO and PVME, the systems previously studied by our group, each repeat unit contained only one hydrogen acceptor site (interacting unit): the $COOCH_3$ ester acceptor group in PMMA, the CH_2-O-CH_2 ether acceptor group in PEO and the $C-O-CH_3$ ether acceptor group in PVME, respectively. In all blends, PVPh bears the only hydrogen bond donor site, the OH moiety. Therefore, for the PVPh/PMMA, PVPh/PEO and PVPh/PVME blends, the mole fraction equated to the donor–acceptor fraction, referred to as 'mole fraction interacting group' in Table 2. In the case of PVPh/PET blends, as each repeat unit of PET bears two ester groups which behave as hydrogen bond acceptors, molar fractions may not be appropriate. In fact, each ester may be counted as one interacting unit (although bearing two oxygen atoms, it has been shown previously that hydrogen bonding mainly involves the carbonyl oxygen atoms of the PET ester groups in PVPh-PET blends [15]). Therefore, in the specific case of PVPh/PET, for each interacting unit of PVPh (hydrogen donor) there are two interacting units of PET available (hydrogen acceptor) per repeat unit. Using the molar fraction of interacting groups, the 71 mol% PVPh composition is equivalent to 55 mol% of interacting PVPh units, a position closer to that where a maximum in the orientation function was observed for PVME and PEO blends with PVPh. In terms of absolute orientation values of PVPh, orientation would be similar to that observed for low draw ratios in PVME-based blends, while it would be lower than that observed for PEO-based blends.

No miscible PET blends have been studied, orientation-wise, to our knowledge. The second component of PVPh-based blends, however, can be compared to PET, as reported in Table 2. Similar compositions, in terms of molar fraction, have been measured only for PVPh-PVME blends. This system yielded a slightly lower orientation factor $\langle P_2(\cos\theta)\rangle$ (0.05 for the 34 mol% PVME blend at $T_g + 15$ versus 0.09 at $T_g + 17$ in the present study). If comparing on a molar fraction of interacting groups basis, however, more blends have been studied with comparable compositions, and range from 0.09 for PVME to 0.16 for PMMA. Nevertheless, it is important to note than orientation reported for the PVPh-PMMA system was determined at $T_g + 10$, that is, at lower temperature, so higher orientation values are to be expected.

Comparing with pure PET is also difficult due to the crystallinity of this polymer. PET can be obtained and oriented in an amorphous form, but it often undergoes stress-induced crystallisation, especially at draw ratios higher than 2.0. Experimental values for *trans* segments of the amorphous phase vary between 0.25 and 0.4 [2,16]

Table 2
Comparison of orientation functions of the hydrogen bond acceptor polymer in PVPh-based blends for $\lambda = 3.5$

Polymer	Mol fraction polymer repeat units	Mol fraction interacting group	$\langle P_2(\cos\theta)\rangle$	T_{draw}
PET[a]	0.29	0.45	0.09	$T_g + 17$
PMMA	0.50	0.50	0.16	$T_g + 10$
PVME	0.34	0.34	0.05	$T_g + 15$
PVME	0.47	0.47	0.09	$T_g + 15$
PEO[b]	0.41	0.41	0.11	$T_g + 15$

[a] Values for the PVPh-PET blend were taken at $\lambda = 3.4$.
[b] Values for the PVPh-PEO blend were taken at $\lambda = 3.0$.

which is considerably higher that the maximum value of 0.05 observed in the present case for the same draw ratio. This could be related, at least in part, to differences in drawing conditions (molecular weight of polymer, temperature and deformation rate). It is also noteworthy that the lowest value was reported using polarization modulation linear dichroism, a technique which allows dynamical measurements during drawing and subsequent relaxation, contrarily to most studies in which a quenched sample is measured. In this way, relaxation is limited and observed orientation factors after deformation normally higher. This technique also allows easier detection of stress-induced crystallisation, as this produces, during relaxation, an increase in orientation instead of the usual decrease. This value is therefore proposed to be more reliable for the amorphous phase. Nevertheless, even if taking into account that more relaxation has occurred in the present case, the orientation value of the *trans* segments of PET in the blends are considerably lower than that reported for the pure polymer. This indicates that blending a relatively rigid polymer such as PET with a polymer having a more flexible, polyethylene-like backbone, therefore can lead to a decrease in the observed orientation of the rigid chain. Whether this decrease stems from some form of cooperativity during deformation or cooperativity during relaxation remains, however, to be assessed. The effect of the bulky, hydrogen bond forming phenolic side-chain could also play a non-negligible role in both processes.

3.3. Blend model construction and validation

Orientation simulations have been shown to yield insights on the deformation phenomenon although the modelling techniques used to simulate deformation do not reproduce adequately the actual deformation process. Recent modelling simulations indicate that PET deformation follows the pseudo-affine or aggregate deformation model [12,13], whereas a significant deviation from this behaviour is predicted from atomistic simulations for PVPh [17]. It is therefore of interest to test whether such a difference may exist in deformation simulations for chains of PVPh and PET in a blend. If the difference on deformation-induced orientation of these two types of chains is maintained in the blends, completely different relaxation times would be required to explain the observed similarity in orientation functions. This would indicate limited chain cooperativity, contrarily to what would be expected for a strongly interacting blend. It has been shown, using polarization-modulation infrared linear dichroism, that relaxation of polystyrene-poly(phenylene oxide) blends was strongly cooperative [4], whereas that of poly (styrene)-poly(vinyl methyl ether) blends was not [5]. However, the behaviour of the latter blend has been shown to be strongly influenced by partial phase separation [8], and this observation therefore does not indicate that blends miscible at the molecular level can present an absence of cooperativity.

The first difficulty for simulating orientation is to get a representative model of the blends. We have recently shown that the Meirovitch building approach can yield reasonable but not perfectly homogeneous models of blends of PVPh with PVME [27]. This procedure does not, however, allow the system to visit all possible states, and is not useful for miscibility predictions. The most straightforward techniques to assess validity of the resulting models and degree of chain intermingling achieved, apart from visual evaluation, have been proposed to be the evaluation of X-ray scattering profiles, which can be compared to experimental curves, and pair distribution functions for main chain atoms as well as for oxygen atoms, as the latter is indicative of hydrogen bonds in the blend. A more quantitative estimation for hydrogen bonding can also be made via geometry considerations.

Fig. 5 shows drawing of a typical model, in its isotopic and in its deformed state, as a superposition of a single chain and a packed cell. The PVPh chain is depicted in gray, whereas the PET chain is in black. Both types of chains are fairly dispersed in the packed cell, although some areas present a distinct predominance of PVPh, as expected from statistical considerations for a 61 wt% (72 mol%) PVPh blend. Single chains vary considerably in their compactness,

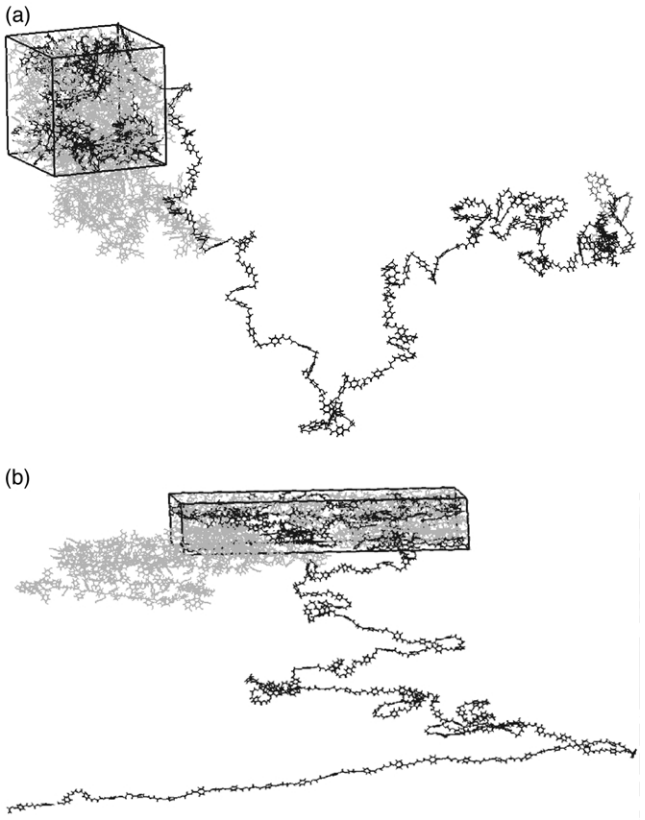

Fig. 5. PVPh-PET amorphous cell model depicted as a combination of packed cell and single chain (PVPh in gray, PET in black) (a) isotropic model, (b) $\lambda = 3.0$.

however, PVPh appearing as a coiled chain whereas PET adopts a much more open conformation, which is attributed to the differences in chain conformational rigidity. After deformation, the two different polymers remain dispersed in the cell, and the isolated PVPh coil appears flattened, whereas, for PET, long and relatively straight polymer chain sections have become aligned with the draw direction.

A typical example of X-ray scattering profile simulation appears in Fig. 6, along with an experimental curve of a 60 wt% PVPh blend measured at 25 °C. As can be seen, simulations reproduce the position of the scattering halos appearing at approximately 18 and 38°. This indicates that the models represent satisfactorily experimental data. The peaks in the experimental curve are considerably broader than those simulated from the models. This difference is attributed to thermal motion, which is not accounted for in the simulated spectrum.

Pair distribution functions are reported in Fig. 7 for intrachain contacts of a typical blend model. As expected, the strongest peaks lie near 1–2 Å, and are related to atom connectivity. Smaller peaks appear between 2 and 4 Å, due to atomic pairs without connectivity in the spatial vicinity. At higher distances, the pair distribution function tends towards zero, in agreement with the absence of long-range order in an amorphous cell.

Intermolecular pair distribution functions appear in Fig. 8(a) for C–C pairs. PVPh-PVPh correlations tend towards 1.0, as expected. For PET-PET correlations, a non-typical behavior is observed, with little correlations at small distances and constant correlations thereafter, which could be related to the more open conformation of the chain and to its small concentration with regards to PVPh. Finally, for the PVPh-PET correlations, values are much larger than for PVPh-PVPh and are, at distances above 10 Å, larger than those of PET-PET. As it has been shown that higher values than both pure polymers correlate with a considerable degree of chain intermingling, it can be concluded that the

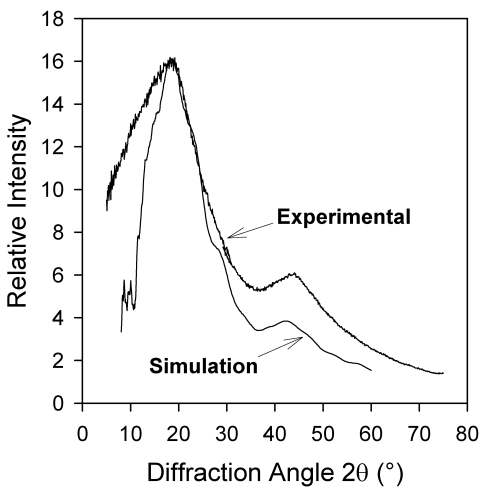

Fig. 6. Comparison between X-ray patterns for an experimental sample and simulation for a typical 61 wt% PVPh blend.

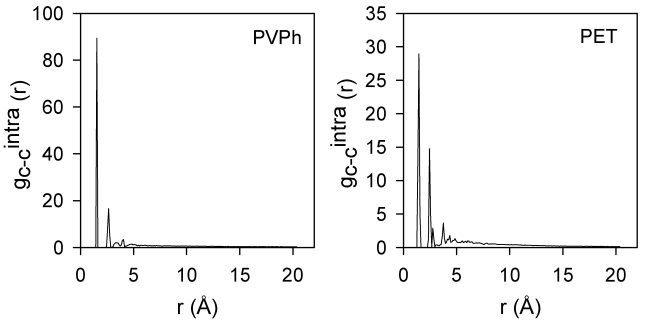

Fig. 7. Intramolecular pair distributions for carbon–carbon pairs of a 61 wt% PVPh blend (average over all models).

models represent a state of miscibility at the molecular level. The g(r) values reach 1.0 for PVPh-PET, but this is not the case neither for PVPh-PVPh nor for PET-PET, which is attributed to a model size effect, in accordance with the work of Stevensen, McCoy, Pimpton and Curro [28]. Composition fluctuations at length scales in excess of 20 Å could also explain in part this observation, in particular of PVPh-PVPh contacts, and related to occurrence of PVPh predominant domains as observed visually.

O–O atom pairs, which appear in Fig. 8(b), show a strong peak near 3.0 for PVPh-PVPh and PVPh-PET, which corresponds to a hydrogen bond distance. This peak is

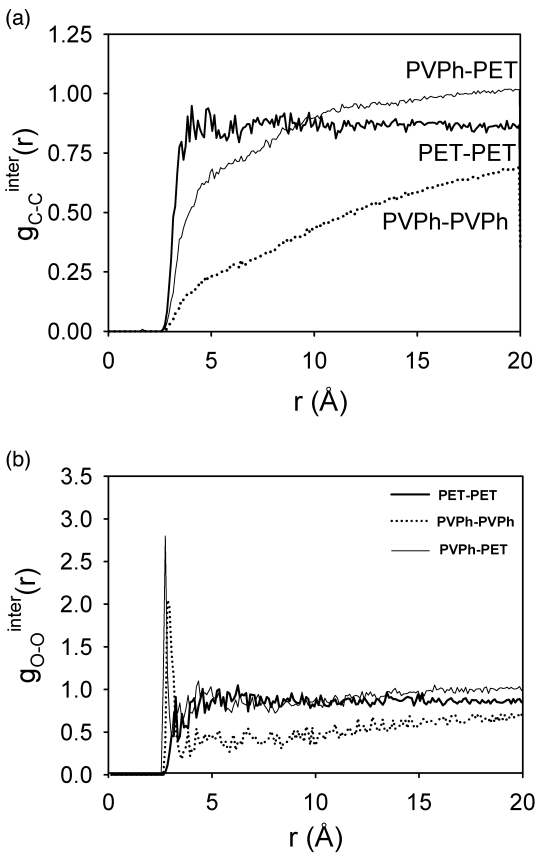

Fig. 8. Intermolecular pair distribution between PVPh and PET chains in the blend model (average over all models) (a) C–C backbone pairs, (b) O–O pairs.

Table 3
Hydrogen bond distribution

Polymer	Model #	Intrachain PVPh-PVPh	Intrachain PVPh-PVPh average	Interchain PVPh-PVPh	Interchain PVPh-PVPh average	Interchain PVPh-PET	Interchain PVPh-PET average	Total	Total average
PVPh			40 ± 20%		20 ± 20%				60 ± 10%
61 wt%PVPh	1	24.8	20 ± 10%	38.4	40 ± 10%	7.2	7 ± 4%	70.4	60 ± 20%
	2	16		32		8.8		56.8	
	3	19.6		40.4		5.6		65.6	
		Interchain[a] PVPh-PET C=O	Interchain[a] PVPh-PET average	Interchain[a] PVPh-PET C–O–C	Interchain[a] PVPh-PET average				
61 wt%PVPh	1	9.0	8 ± 3%	0	1 ± 2%				
	2	9.0		2.0					
	3	6.5		0.5					

[a] Calculated versus the number of available C=O or C–O groups in PET.

higher for PVPh-PET than for PVPh-PVPh, whereas it is broader in the latter case. In both cases, the occurrence of a prominent peak in this position clearly indicates that hydrogen bonds occur and that the chains of PVPh and PEO are in close contact.

Hydrogen bond quantification via geometrical considerations is reported in Table 3. Within experimental error, PVPh-PVPh hydrogen bonds appear non-affected by the presence of PET. This was also the case for the previously modelled PVPh-PVME blend. PVPh-PET hydrogen bonding is modest but significant, with 8% of the sp^2 ester oxygens and 1% of the sp^3 ester oxygens of PET involved in hydrogen bonds with PVPh. This observation is in agreement with FTIR investigations of a 50 mol% PVPh-PET blend [15], which showed that carbonyl groups were forming hydrogen bonds more readily than sp^3 oxygens of the ester *groups*, although no quantitative comparison can be made since the composition (50 mol%) is different from that studied here (40 wt% or 29 mol% PET). In spite of the lack of experimental data for PVPh/PET specifically, there is conclusive evidence in the literature that the C–O–C group can also be a hydrogen bond acceptor. The works of Coleman and coworkers [29] and Qin et al. [30] on PVPh/PEO and PVPh/PVME using FTIR spectroscopy demonstrate that hydrogen bonds can be formed between the hydroxyl moiety of PVPh and the ether oxygen of the PEO/PVME.

The fact that the $g^{\text{inter}}_{\text{O-O}}$ peak corresponding to hydrogen bonds is large with respect to the number of PVPh-PET hydrogen bonds actually calculated indicates that a number of ester groups are in close proximity to hydroxyl atoms, although the geometry is not good enough for them to qualify as hydrogen bonds.

3.4. Deformation simulations of blends

Deformation of the models was performed using a Parrinello–Rahman [31] deformation scheme. This method has been discussed in more details previously [13–14], and gave, for pure PET, results comparable to an alternate deformation scheme proposed in the literature [12]. It is however far from accurately reproducing the forces acting on the polymer chains in a classical fiber drawing experiment: All atoms are subjected to deformation, contrarily to experimental conditions where the force is mostly transmitted via backbone atoms. Experimentally, on the other hand, stress is applied to the sample extremities, and is propagated through the polymer backbone and surrounding chains. Hence, all atoms may not experience the same stress. Further, the deformation scheme is similar to that of roll-drawing, with lateral stresses applied simultaneously to a uniaxial stretching in the machine direction, and a constant stress is applied, as in a creep experiment. Deformation proceeds much faster than in the actual experiments, and varies with time and deformation ratio attained. A deformation typically takes 5 ps to reach a λ value of 2, which means that the deformation rate is non-linear, and proceeds faster at deformation onset, becomimg smaller and eventually, falling to zero upon reaching the target stress. Speed is of the order of 500 m s^{-1} at the deformation midpoint. This is considerably faster than the experimental deformation rate, which varies exponentially, is of 0.1 s^{-1}, for which the λ value of 2 is reached in 7 s. Nevertheless, variations in the rates were previously performed on pure PET and on pure PVPh by varying the 'cell mass' w in the Parrinello–Rahman technique. No change was observed in orientation of conformer populations, within estimated error, for a given deformation ratio value. This indicates that the deformation speed is not an important factor for deformation-induced orientation, and is in agreement with the interpretation generally held that deformation speed results in changes in orientation due to changes in relaxation. Indeed, the time needed to deform a sample to a λ of 2.0, which is 5 ps, is orders of magnitude below the

first relaxation time of the Doi-Edwards model, or Rouse equilibrium relaxation time, which has been measured as 8 s at a temperature of 85 °C for PET [2], a value which is probably slightly overestimated due to the limited data measurements short deformation times. On the other hand, the time required to stretch the sample (approximately 7 s for a λ of 2.0), coupled with the time needed to perform the quenching (from 2 to 4 s), is of the same order of magnitude as this first relaxation time. This clearly indicates that experimental data incorporate the effect of Rouse relaxation, which lowers observed orientation, whereas the simulation does not take into account this effect.

Because of these differences with experimental conditions, and because of the number of approximations made, such simulations are proposed neither to represent accurately the deformation process nor to be useful for mechanical property calculations. They are mainly used to get insights on the possible deformation mechanism, when freed from most relaxation interferences, which is not possible at this time experimentally due to time limits of the available techniques.

Deformation was performed for the three models built, and a typical example of a deformed cell appears in Fig. 5(b). Chains appear to align with the deformation direction, more *trans* segments appear, but chain loops comprising other conformations are still clearly present.

If one follows the conformation population evolution with drawing, as reported in Fig. 9, a significant and continuous decrease in *gauche* segments is observed for both polymers in the blend, as was also observed in deformation simulations of both pure polymers [12,14] as well as in experimental data reported for pure PET [2,16,19]. In both cases, *trans* population first slightly decreases and increases thereafter, reaching or exceeding values observed in the isotropic models. Non-*trans*-non-*gauche* segment population increases substantially in PVPh, whereas it stays relatively constant in PET. As these are generally higher-energy conformations, this indicates that PVPh appears to have more difficulty in deforming, which is attributed to the presence of the bulky phenol side-group in the repeat unit.

We also studied the evolution of the individual energy components of the system during the deformation process. Fig. 10 shows the change in bond, angle, torsion and non-bonded energy components for a typical PVPh/PET model as function of the draw ratio. It can be seen that the more dramatic change in energy occurs at the beginning of the deformation process, which corresponds to a notorious change in *gauche* conformer population for PET and to changes in all conformers for PVPh (see Fig. 9). Between $\lambda = 2-2.5$ up to $\lambda = 2.8$, a stabilisation of the different energy components is observed, in spite of observing changes in the conformer fractions. This can be attributed to the fact that although there is an increase in low energy *trans* conformers, there is also a very important increase in high energy non-*trans*, non-*gauche* conformers. For draw ratios beyond 2.8, we can observe that the torsion energy begins to

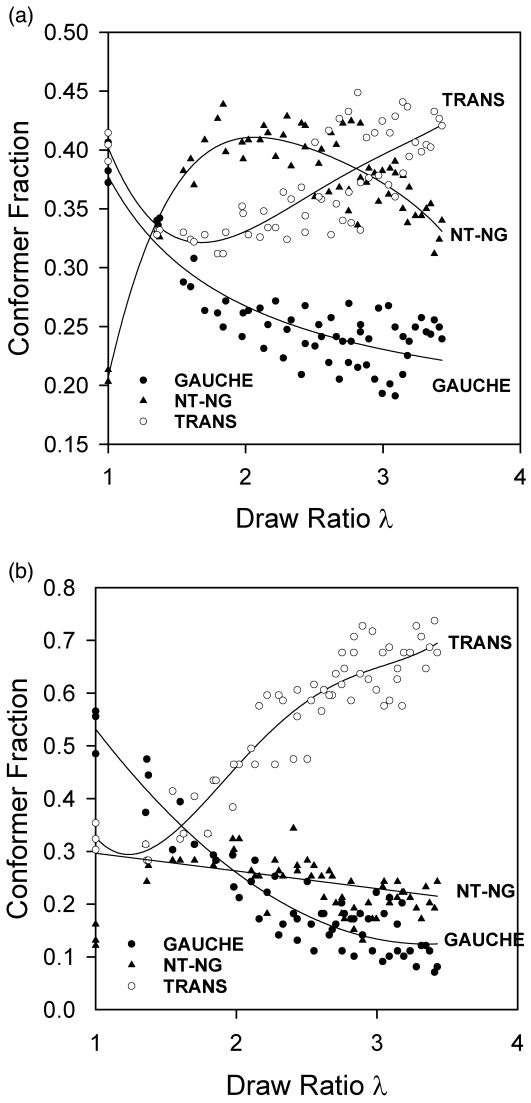

Fig. 9. *Trans*, *gauche*, non-*trans*, non-*gauche* segment fraction changes versus draw ratio. (a) PVPh, (b) PET.

decrease, whereas all the other energy components remain stable. This could tentatively be explained due to the marked fall in number of non-*trans*, non-*gauche* conformers for PVPh in favour of *trans* conformers, which have a lower energy.

Conformational changes allow chain segments to orient along the machine direction, and resulting polymers become oriented, as was seen in Fig. 5. As orientation depends on segmental definition, and as for PET this effect is particularly important, for the simulations, various groups were used to follow the orientation changes. For PVPh, only the backbone segments, as defined in Fig. 11, were used. For PET, glycol C–C segments as well as aromatic rings were followed. For aliphatic chains of both polymers, distinction was made for *trans*, *gauche* and non-*trans*, non-*gauche* segments. Orientation data for all backbone segments, irrespective of conformations, are reported in Fig. 12. As expected from the limited relaxation present in the models,

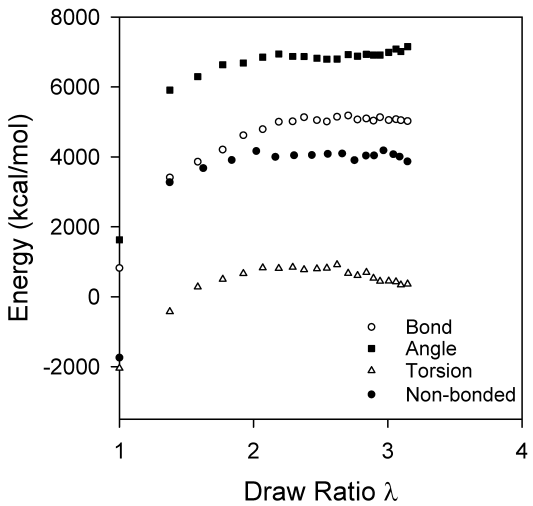

Fig. 10. Changes in individual energy terms with draw ratio.

experimental values are considerably lower than modelled ones. Contrarily to experimental data, orientation curves are not linear with respect to draw ratio. Orientation of PET in the modelled blend is similar to that observed previously for pure PET modelling. Therefore, blending these chains does not seem to affect the way they behave upon deformation. If the modelling represents accurately reality, this would mean that the experimentally observed similarity in orientation of PET and PVPh chains would arise from differences in relaxation of these two types of chains.

A point that naturally arises when discussing the discrepancy between experimental and simulated results is the difference in the respective molecular weights of the blends. In the experiments, the molecular weight of PVPh is of about 5,200 g mol^{-1} and of 30,000 g mol^{-1} in the modelling. In the case of PET, a value of 54,600 g mol^{-1} was reported for the experimental samples, while the simulated molecules had a M_w of 19,200 g mol^{-1}. Molecular weights for modelling experiments were chosen, in order to minimize calculation times, as the minimum molecular weights

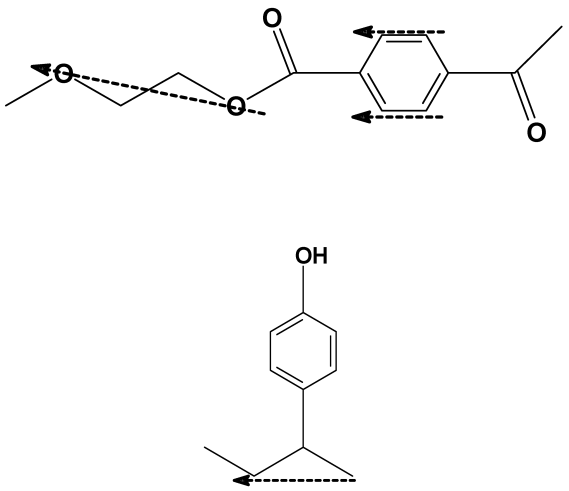

Fig. 11. Definition of segments used for orientation determination.

that allowed to respect to the correlation length, which is the persistence length for static experiments, but which was proposed by our group to be the distance between entanglements for deformation experiments, on the basis of the importance of entanglements in both the deformation and relaxation as discussed in more details previously [13,14]. On the other hand, for experimental measurements, limitation stemmed from the available molecular weights, which did not match the modelling requirements. This difference is very relevant, as it has been reported either experimentally [32] and theoretically [33] that final orientation of the samples is molecular weight dependent.

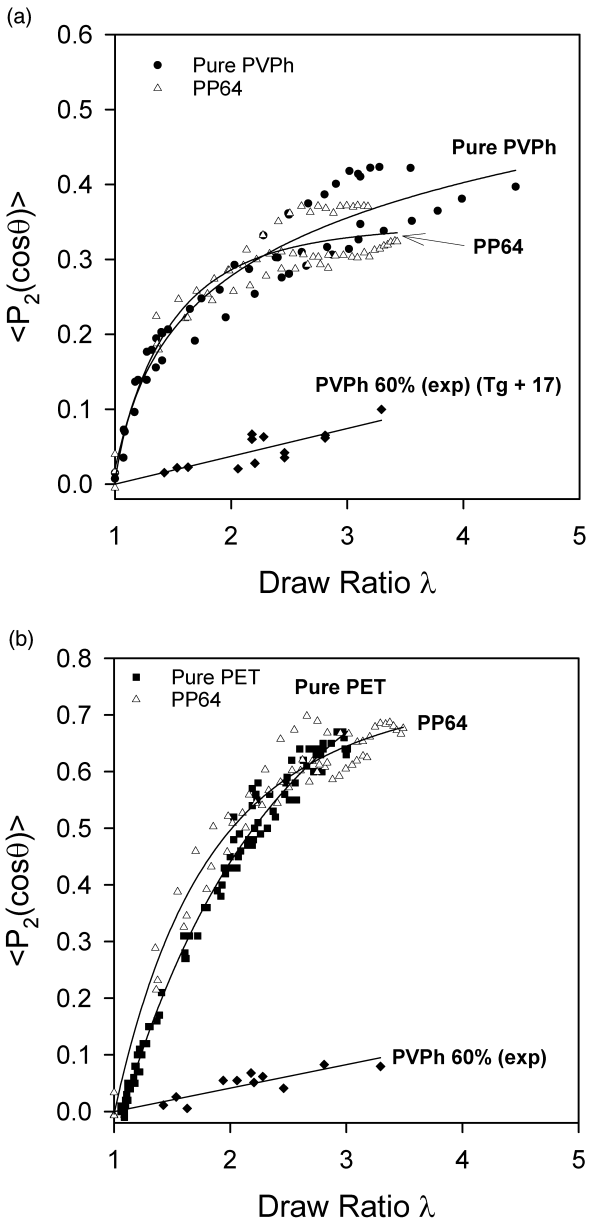

Fig. 12. Uniaxial orientation versus draw ratio for experimental, $T_g + 17$ and 0.1 s^{-1} for blends and simulated data, $T = 298$ K, in pure form and in blends. (a) PVPh chains (experimental $T_g + 17$ and 0.1 s^{-1} for blends, modeling taken from Ref. [14]) (b) PET chains (experimental $T_g + 17$ and 0.1 s^{-1} for blends, modelling taken from Ref. [13]).

Nevertheless, it is also important to point out that it has been proposed that molecular weight plays a role in the relaxation process only for the second and third relaxation times [33]. Due to the short times available during the computer simulation, the modelling results presented here are well within the first relaxation (Rouse) time, where the orientation is unaffected by molecular weight. Therefore, the fact that the chain size of the simulated molecules do not match the experimental ones does not explain the difference between both results.

If one looks at orientation of individual conformers in the blends, as reported in Fig. 13, for both polymers, considerable data dispersion is observed, which is attributed to the limited size of the models. *Trans* orientation is however clearly higher for both PET and PVPh chains, non-*trans*, non-*gauche* having an intermediate value and *gauche* segments having the lowest orientation, as was also reported for pure PVPh and pure PET. *Gauche* segments have a similar orientation for both chains in the blend, contrarily to *trans* segments which reach values near 0.8 in PET and of only 0.42 in PVPh. A similar trend was observed for pure PET and pure PVPh, although slightly higher values were observed for *trans* segment orientation in pure PVPh. Other segments were, within error, comparable. The fact that simulated orientation is similar for PVPh and PET chains in pure polymer as compared to blend, could be related to the limited number of hydrogen bonds observed for this blend composition. However, this may also be an intrinsic property of deformation, upon which forces exerted on the chains are probably sufficient to break local interactions such as hydrogen bond, which may break and reform dynamically during deformation. On the other hand, relaxation proceeds without input of additional high energy, and interactions may therefore then play a more prominent role (Fig. 13).

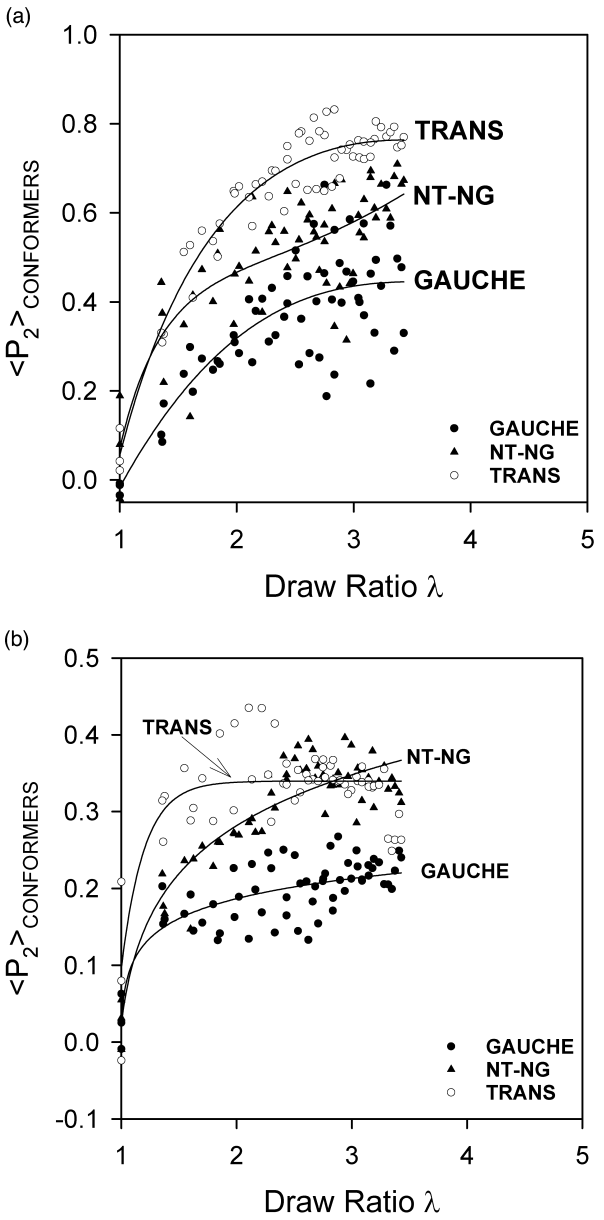

Fig. 13. *Trans*, *gauche*, non-*trans*, non-*gauche* and backbone orientation versus draw ratio (a) PVPh, (b) PET.

4. Conclusion

In the present work, the effect of backbone chain rigidity differences on orientation in a miscible PVPh-PET blend was investigated. Experimental evaluation of orientation showed that, at low PET concentrations, orientation was not detectable, but increased substantially and became measurable for a 60 wt% (71 mol%) PVPh blend. Computer simulations indicate that, in this specific case, the deformation-induced orientation is different for the two polymers. This is attributed to different chain rigidities, which could be defined as the number of rotatable bonds leading to changes in the chain length. As the same final orientation was measured, it is proposed that relaxation should not proceed at the same rate for PET and PVPh chains in the blend. This would be consistent with the fact that a different proportion of atoms are involved in hydrogen bonds in both chains. Relaxation may occur more rapidly in the blends as compared to the pure polymer due to a more disorganised local environment of the chains. Experimental measurements of chain relaxation in these blends are clearly needed to confirm these hypothesis, and will be the object of future work.

Acknowledgements

This research was supported by the NSERC (Natural Sciences and Engineering Research Council of Canada), and by the FCAR (Fonds pour la Formation de Chercheurs et l'Aide à la Recherche, now called FQRNT or Fonds québécois de la recherche sur la nature et les technologies). K.C. Cole, of the Institut for Industrial Materials (IMI) in

Boucherville, Québec, Canada, is also thanked for specular reflection measurements. Technical help of S. Groleau, of the CERSIM in Université Laval, for FTIR dichroism is also gratefully acknowledged. One of the authors, P. Gestoso, also acknowledges the support of the scholarships from the Ministère de l'Éducation du Québec and from Université Laval.

References

[1] Oultache AK, Kong X, Pellerin C, Brisson J, Pézolet M, Prud'homme RE. Polymer 2001;42:9051.
[2] Duchesne C, Kong X, Brisson J, Pézolet M, Prud'homme RE. Macromolecules 2002;35:8768.
[3] Messé L, Prud'homme RE. Polymer 2001;42:563.
[4] Messé L, Prud'homme RE. J Polym Sci, Polym Phys Ed 2000;38: 1405.
[5] Pellerin C, Prud'homme RE, Pézolet M. Macromolecules 2000;33: 7009.
[6] Jasse B, Tassin J-F, Monnerie L. Prog Colloid Polym Sci 1993;92:8.
[7] Zhao Y, Prud'homme RE, Bazuin CG. Macromolecules 1991;24: 1261.
[8] Pellerin C, Prud'homme RE, Pézolet M. Polymer 2003;44:3291.
[9] Li D, Brisson J. Macromolecules 1997;30:8425.
[10] Rinderknecht S, Brisson J. Macromolecules 1999;32:8509.
[11] Gestoso P, Brisson J. Polymer 2001;42:8415.
[12] Zhou J, Nicholson TM, Davies GR, Ward IM. Comput Theor Polym Sci 2000;10:43.
[13] Roberge M, Prud'homme RE, Brisson J. Polymer, submitted for publication.
[14] Gestoso P, Brisson J. J Polym Sci, Polym Phys Ed 2002;40:1601.
[15] Landry CTJ, Massa DJ, Teegarden DM, Landry MR, Henrichs PM, Colby RH. Macromolecules 1993;26:6299.
[16] Nobbs JH, Bower DI, Ward IM. J Polym Sci, Polym Phys 1979;17: 259.
[17] Gestoso P, Brisson J. Comput Theor Polym Sci 2001;11:263.
[18] Hevenqvist MS, Bharadwaj K, Boyd RH. Macromolecules 1998;31: 1556.
[19] Cole KC, Guévremont J, Ajji A, Dumoulin MM. Appl Spectrosc 1994;48:1513.
[20] Li D, Brisson J. Polymer 1994;35:2078.
[21] Maple JA, Hwang M-J, Stockfisch TP, Dinur U, Waldman M, Ewig CS. J Comput Chem 1994;15:162.
[22] Gestoso P, Brisson J. Comput Theor Polym Sci 2001;11:263.
[23] Meirovitch HJ. Chem Phys 1983;79:502.
[24] Li Y, Mattice WL. Macromolecules 1992;25:4947.
[25] Zhang M, Choi P, Sundararaj U. Polymer 2003;44:1979.
[26] Li D, Brisson J. Macromolecules 1996;29:868.
[27] Gestoso P, Brisson J. Polymer 2003;44:2321.
[28] Stevenson CS, McCoy JD, Pimpton SJ, Curro JB. J Chem Phys 1995; 103:1200.
[29] Moskala EJ, Varnell DF, Coleman MM. Polymer 1985;26:228.
[30] Qin C, Pires ATN, Belfiore LA. Polym Commun 1990;31:177.
[31] Parrinello M, Rahman A. J Phys (Paris) 1981;C6:511.
[32] Jasse B, Tassin J-F, Monnerie L. Prog Colloid Polym Sci 1993;92:8.
[33] Doi M, Edwards SF. J Chem Soc, Faraday Trans 1978;74:1789. see also p 1802, 1818.